Nonlin. Processes Geophys. Discuss., doi:10.5194/npg-2016-49, 2016
Manuscript under review for journal Nonlin. Processes Geophys.
Published: 27 September 2016
© Author(s) 2016. CC-BY 3.0 License.

Nonlinear Processes in Geophysics
Discussions
Open Access
EGU

Slow strain waves in blocky geological media from GPS and seismological observations on the Amurian plate

V.G. Bykov and S.V. Trofimenko

Institute of Tectonics and Geophysics, Far Eastern Branch, Russian Academy of Sciences,
65, Kim Yu Chen St., Khabarovsk, 680000, Russia
Correspondence to: V.G. Bykov (bykov@itig.as.khb.ru)

Abstract. Based on the statistical analysis of spatiotemporal distribution of earthquake epicenters and perennial geodetic observation series, new evidence is obtained for the existence of slow strain waves in the Earth. The results of our investigation allow us to identify the dynamics of seismicity along the northern boundary of the Amurian plate as a wave process. Migration of epicenters of weak earthquakes ($2 \le M \le 4$) is initiated by the east-west propagation of a strain wave front at an average velocity of 2.7 km/day. We have found a synchronous quasi-periodic variation of seismicity in equally spaced clusters with spatial periods of 3.5° and 7.26°comparable with the length of slow strain waves. The geodetic observations at GPS sites in proximity to local active faults show that in a number of cases, the GPS site coordinate seasonal variations exhibit a significant phase shift, whereas the time series of these GPS sites differ significantly from a sinusoid. Based on experimental observation data and the developed model of crustal block movement we have shown that there is one possible interpretation for this fact that the trajectory of GPS station position disturbance is induced by migrating of crustal deformation in the form of slow waves.

Key words: background seismicity, seismic clusters, strain waves, Amurian plate, space-time seismicity model, oscillatory movements of crustal blocks.

Nonlin. Processes Geophys. Discuss., doi:10.5194/npg-2016-49, 2016
Manuscript under review for journal Nonlin. Processes Geophys.
Published: 27 September 2016
© Author(s) 2016. CC-BY 3.0 License.

1 Introduction

The inhomogeneous blocky structure of the crust and the lithosphere considerably affects the deformation, seismic, filtration and other processes. The effect of the blocky structure on the distribution of earthquakes can be especially clearly traced. It is exactly the blocky structure of the geological medium which results in the generation of waves of different types including slow strain waves (Bykov, 2008). Clarification of the link between movements of tectonic structures and slow strain wave processes is of fundamental importance for expanding our understanding of the physics of earthquakes.

The most important problem of recent geodynamics is to clarify the mechanisms responsible for the propagation of the energy of deformation processes and tectonic stress transfer at the boundaries between the blocks and the lithospheric plates, and to explore the causes of migration of earthquake epicenters. The problem has been argued for more than 45 years since Elsasser's publication (1969), suggesting the equation of local stress transfer in the rigid elastic lithosphere underlain by the viscous asthenosphere. The possibility of using Elsasser's model to describe migration of seismicity was further discussed in papers published by other researchers. Bott and Dean (1973) introduced the term "stress or strain waves" and obtained the expression for the velocity of the wave propagating along the lithospheric plate. According to their calculation, the stress wave velocity attains to 0.1-100 km/yr. Anderson (1975) generalized Elsasser's model in order to elucidate the mechanism of earthquake migration in the subduction zone and estimated the stress wave velocity along the island arc about 50-170 km/yr. In the model developed by Ida (1974), the solution was obtained in the shape of "slow-moving deformation pulses" propagating along the fault at a constant velocity. The gouge viscosity and thickness variations in the fault yield the pulse velocity ranging from 10-100 km/yr to 1-10 km/day. The first interval corresponds to earthquake migration velocities at a wavelength of about tens of kilometers, whereas the second interval is compliant with aseismic creep at about 1 km wavelength. Scholz (1977) introduced the concept of the "deformation front" to describe large-scale tectonic processes triggering large earthquakes. As estimated by Scholz, the velocity of the deformation front propagating through NE China, that triggered the 1975, M=7.3 Haicheng earthquake, attained to 110 km/yr.

The advances in theoretical studies of slow strain waves in the Earth initiated the search for the possibilities of experimentally detecting the propagation effects of the waves of this type, and, in the first place, the intense study of earthquake migration. By now, the deformographic, geodetic and hydrological measurements performed worldwide have revealed the migration of deformations at velocities of about 10-100 km/yr and 1-10 km/day (Kasahara, 1979; Bella et al., 1990; Harada et al., 2003; Kuz'min, 2012; Reuveni et al., 2014; Yoshioka et al., 2015).

Nonlin. Processes Geophys. Discuss., doi:10.5194/npg-2016-49, 2016
Manuscript under review for journal Nonlin. Processes Geophys.
Published: 27 September 2016
© Author(s) 2016. CC-BY 3.0 License.

Migration of earthquake epicenters coincides with the velocity (10-100 km/yr) and direction of crustal deformation movement (Kasahara, 1979; Barabanov et al., 1988) and with hydrological effects (Kissin, 2008). Furthermore, the absorption and dispersion of the waveforms of migrating deformation were detected (Kasahara, 1979; Barabanov et al., 1988), i.e., the main properties of a common wave process. In terms of the physical mechanism of propagation, slow strain waves are similar to common seismic waves, but the fundamental difference is that they propagate at super low velocities, ultra low frequencies and have large wavelength (Bykov, 2005). This hampers the direct instrumental measurements of strain waves and the concomitant effects.

In the present study, we have obtained new evidence of the existence of strain waves in the Earth resting upon a comprehensive statistical analysis of the dynamics of seismicity along the northern boundary of the Amurian plate and the data derived from in situ GPS experimental observations performed near this boundary.

2 Methods for detection of slow strain waves

Slow strain wave transmittance through the fault-blocky geological medium is accompanied by various seismic, hydrogeological, electrokinetic, geochemical and other effects. The methods for strain wave detection are divided into indirect, that display the wave-shaped variations in the geophysical fields due to temporal variations of the stress state of the medium, and direct ones immediately recording the migration of deformations.

The seismic, geoelectric and geochemical methods of strain wave recording are referred to the indirect methods. Indirect evidence of the existence of strain waves is manifested in the targeted migration of large earthquakes (Stein et al., 1997), the occurrence of seismic velocity anomalies (Lukk and Nersesov, 1982; Nevskii et al., 1987), a cyclic wandering of aseismic strips in the Earth's mantle (Malamud and Nikolaevsky, 1983; 1985); oscillatory movements of the seismic reflection sites (Bazavluk and Yudakhin, 1993; Bormotov and Bykov, 1999) and the migration of geophysical field anomalies (radon, electrokinetic signals) in proximity to faults (Nikolaevskiy, 1998).

The direct indications of strain waves are displayed in wave fluctuations of the ground water level and the migration of slopes and surface deformations. The direct methods exploring temporal variations of crustal deformation comprise the deformographic (Kasahara, 1979; Ishii et al., 1983; Nevskii et al., 1987; Bella et al., 1990; Harada et al., 2003), hydrogeodynamic (Barabanov et al., 1988; Kissin, 2008) and geodetic measurements (Kuz'min, 2012) including the methods of deformation measurements using laser ranging (Milyukov et al., 2013) and GPS observations (Reuveni et al., 2014; Yoshioka et al., 2015).

Nonlin. Processes Geophys. Discuss., doi:10.5194/npg-2016-49, 2016
Manuscript under review for journal Nonlin. Processes Geophys.
Published: 27 September 2016
© Author(s) 2016. CC-BY 3.0 License.

To detect the main physical mechanisms of seismicity migration and the generation of signals of different nature that are accompanying strain waves, we need performing further observations and improving GPS- and seismological data processing technique, and conducting theoretically prepared and purposeful experiments.

The answer to the question "where to search for slow strain waves?" is directly linked with the detection of the main types of tectonic structures generating these waves.

3 Tectonic structures generating slow strain waves

From the published results it follows that subduction, collision, active riftogenesis and transform fault zones are the most probable types of tectonic structures generating strain waves. These intensive sources of different tectonic nature possess a common property – they are the interaction zones between crustal blocks and the lithospheric plates.

Migration of shear deformation in subduction zones is directed from the ocean toward the coast. This general tendency was first revealed in area of the Japan island arc where migration is oriented east-west, and in the opposite Pacific coastal area – in the western Cordilleras, where deformations migrated from south to north (Kasahara, 1979). Migration of the maximum of the vertical crustal deformation from the subduction zone toward the continent at a velocity of about 10 km/yr was also observed near the Tohoku region (northeastern Japan) and the Izu Peninsula (central Japan), where the Pacific and Philippine plates subduct beneath the Eurasian plate (Miura et al., 1989). All these data reasonably lead to an assumption that subduction zones are one of the possible sources of slow strain waves.

The seismicity pattern observed in the south of Middle Asia can also be explained by strain waves excited under the oscillating regime of the Eurasian and Indian lithospheric plate collision in the Pamir and Tien Shan junction zone (Nersesov et al., 1990). The compression at the Indostan and Eurasian lithospheric plate boundary in the Himalayan collision zone is the source of "fast" and "slow" waves of plastic deformation that trigger earthquakes in Central and East Asia (Wang and Zhang, 2005).

In the Baikal rift system, four main groups of strain waves with different velocities (7-95 km/yr) and lengths (130-2000 km) are distinguished that cause recent activation of seismoactive faults in Central Asia (Gorbunova and Sherman, 2012).

Based on continuous long-term seismic and laser ranging observation data, it has been established the effect of propagation of slow waves of tectonic deformations traveling along transform faults at velocities of 40-50 km/yr at the lithospheric plate boundaries in Southern California and the Kopet-Dag region (Nevskii et al., 1987). Seismicity variations along the

Nonlin. Processes Geophys. Discuss., doi:10.5194/npg-2016-49, 2016
Manuscript under review for journal Nonlin. Processes Geophys.
Published: 27 September 2016
© Author(s) 2016. CC-BY 3.0 License.

159 Pacific and North American plate boundary in the San-Andreas transform fault zone (California)
160 are also suggested to be associated with "slowly traveling strain waves" (Press and Allen, 1995).
161 The rotational block movements in the fault zones due to tectonic processes or earthquakes
162 are considered one of the main physical mechanisms of strain wave generation (Nikolaevskiy,
163 1996; Lee et al., 2009; Teisseyre et al., 2006).
164
165 **4 Seismic effects of slow strain waves at the northern edge of the Amurian plate**
166
167 In order to specifically investigate the relationship between strain waves and the dynamics
168 and seismicity pattern observed in fault-blocky geological media, we have selected the study
169 area on the northern margin of the Amurian plate – the most seismically active area of the
170 interaction zone between the Amurian and Eurasian plates.
171 The analysis of the spatiotemporal seismicity pattern observed in vast regions is commonly
172 performed based on statistical processing of earthquake catalogues. The directions of earthquake
173 epicenter (or groups of epicenters) displacements are defined and their displacement rates are
174 determined. As opposed to the standard regional approach, we here applied a comprehensive
175 analysis including both conventional statistical methods and those of cluster analysis adapted by
176 the authors for the geodynamic zone gradation. The details of developed clustering technique
177 and statistical analysis of background seismicity can be found in (Trofimenko et al., 2015).
178 To study the dynamics of seismicity in different zones, the area along the northern
179 boundary of the Amurian plate was divided into separate clusters (Fig. 1). When clustering, we
180 applied the criterion of earthquake grouping near active faults, and the geomorphological and
181 tectonic features of active structures, as well as the presence of meridional (submeridional) first-
182 rank faults within the distinguished zones, were taken into consideration.
183 When developing space-time models of seismicity, the spatial relationship between
184 separate seismic clusters during a year was revealed and taken into account. Based on statistical
185 distributions of earthquakes, the analysis of seismicity maxima passage over east-westerly
186 arranged clusters has been performed.
187 The basic data were derived from the catalogue "Earthquakes of Russia"
188 (http://eqru.gsras.ru), the catalogue compiled by the Baikal Branch of the Geophysical Survey of
189 the Russian Academy of Sciences (GS RAS) (http://www.seis-bykl.ru/) and the IRIS catalogue
190 (http://www.iris.edu).
191 As a result of the calculation, the average period of seismicity maximum passage in days
192 from the beginning of the year has been determined for each cluster, which is assigned to the
193 average value of the cluster longitude. These values were used for the calculation of the

Nonlin. Processes Geophys. Discuss., doi:10.5194/npg-2016-49, 2016
Manuscript under review for journal Nonlin. Processes Geophys.
Published: 27 September 2016
© Author(s) 2016. CC-BY 3.0 License.

displacement rate of seismicity maxima. We calculated the velocities and wavelengths of slow strain waves from the maxima of the spatial correlation of seismicity.

The spatiotemporal distributions of earthquake epicenters reflect synchronization of seismicity maxima in the annual cycles over a certain spatial interval (migration period). The statistical calculations performed for each cluster allowed the identification of six similar spatiotemporal cycles of seismicity maxima migration A, B, C, D, E and F (Fig. 1), for which the spatial periods of migration and displacement rates of seismicity maxima have been calculated.

In the northeastern segment, the maxima of statistical distributions are located in the clusters arranged nearly equally apart from each other, at $L_{A-C} = (7.26 \pm 0.74)°$, which corresponds to a distance of 360-420 km for a range of investigated latitudes. For the northwestern segment, the spatial period is equal to $L_{D-F} = (3.8 \pm 0.5)°$, at the average, which corresponds to half of the interval $L_{A-C,}$ or a distance of 210-270 km (Fig. 1). In the study area, the parameter L_{A-C} is equal to double the distance between the main structural-tectonic elements of the Earth's crust and corresponds to double the size of tectonic inhomogeneities revealed from the geophysical field anomalies (Trofimenko, 2010).

The determined spatial period $L_{A-C}=7.26°$ (360-420 km) is comparable with the wavelength λ=250-450 km of slow strain waves observed in the study area on the northern margin of the Amurian plate (Pribaikalya and Priamurye areas lying within 107°E-140°E) (Sherman et al., 2011). The direction of the seismicity maxima displacement coincides with the displacement vector of the strain wave front (Sherman, 2013) (Fig. 2).

The displacement rate values for seismicity maxima are obtained from regression equations using the linear approximation method and are equal to U_A=-2.6 km/day, U_B=-3.2 km/day, U_C=-2.7 km/day, U_D=-2.61 km/day, U_E=-2.83 km/day and U_F=-2.15 km/day for spatial cycles A, B, C, D, E and F, respectively. The minus sign means the westward displacement of the seismicity maxima.

For the entire northeastern segment, the average value of the velocity modulus of the seismicity maxima displacement (with a relative determination error of 7%) is equal to $U_{A-C} =$ 2.75-2.80 km/day, whereas for the northwestern segment this value is $U_{D-F} \approx (2.5 \pm 0.3)$ km/day. The seismicity maxima displacement rate value is $U_{A-F} \approx (2.68 \pm 0.34)$ km/day or about 1000 km/yr along the entire northern boundary of the Amurian plate.

5 The slow strain wave effects inferred from GPS observations

To explore the deformation processes in the geological medium with a discrete blocky structure and to perform special GPS experimental observations, we selected the South Yakutia geodynamic polygon located near the northern boundary of the Amurian plate, at the junction of

Nonlin. Processes Geophys. Discuss., doi:10.5194/npg-2016-49, 2016
Manuscript under review for journal Nonlin. Processes Geophys.
Published: 27 September 2016
© Author(s) 2016. CC-BY 3.0 License.

two major tectonic structures – the Aldan Shield and the Stanovoy Range. Recently, a number of blocks of different size and configuration have been inferred here from geological data. These blocks experience the vertical and horizontal movements of different directions, velocities and amplitudes (Imaeva et al., 2012), which are responsible for a complicated character of tectonic movements.

We have analyzed a set of time series obtained at two of collocated GPS sites NRGR and NRG2 situated near the active fault intersection area in the central part of the Stanovoy Range (Fig. 1). The NRGR site is located in area of the Chulman depression on 15×20 km^2 size microblock and is involved in different types of crustal movements and deformations in consistency with the kinematics of the bordering active faults. The site NRG2 location is approximately 2 km south of the NRGR site and closer to the zone of influence of the active Berkakit fault. The GPS time series obtained at stations NRGR and NRG2 for the horizontal and vertical components are shown in Fig. 3. The stable long-period displacement component is typical for both observation sites in the southeastern direction. For the vertical and horizontal components observed in other directions, the course of the annual displacements is absolutely different. At the two observation sites, the horizontal displacement components in the "North-South" direction are represented by in-phase curves that can be approximated by a sinusoid (Fig. 3 a). The vertical and horizontal displacement components in the "East-West" direction vary in an anti-phase manner during separate periods of measurements (Fig. 3 b, c), which contradicts the common dynamics of long-period components. The shapes of these curves for the horizontal displacement components are appreciably different from a sinusoid.

It is necessary to emphasize that the meteorological factors in the annual cycles influence the shapes of the movement trajectories of the collocated sites equally (van Dam et al., 1994). Therefore, the detected paradox cannot be explained by the meteorological causes.

This paradox can only be resolved in the case when the observation sites are adjacent to the boundaries of specific – "hinge" – type local faults (Fig. 4 a). Really, for the site NRGR, a local feathering fault of the Sunnangyn-Larba northeast-trending fault system is the "hinge", whereas for the site NRG2, the" hinge" is one of the branches of the Berkakit northwest-trending fault (Fig. 1). The physical model of this fault-blocky structure can be represented as a set of rods – physical pendulums (Fig. 4b), whose lower parts are fixed, while the upper parts are disturbed from the equilibrium condition. In this case, the upper parts of the rods (blocks) are displaced with respect to some central line (the fault hinge).

The approximation curve fitting for the vertical component of block displacement has led to one more unexpected result. The shape of the best fit function approximating the experimental curve appeared to coincide with a breather – the solution (2) of the sine-Gordon equation (see

Nonlin. Processes Geophys. Discuss., doi:10.5194/npg-2016-49, 2016
Manuscript under review for journal Nonlin. Processes Geophys.
Published: 27 September 2016
© Author(s) 2016. CC-BY 3.0 License.

below). When selecting the theoretical curve in the shape of a breather (2), this result for the "North-South" component is obtained at $\omega = 0.873$ with an error equal to 0.048 (for the sine 0.069),while for the "East-West" component − at $\omega = 0.780$ with an error equal to 0.052 (for the cosine 0.149). The approximation error of experimental data is calculated from the formula $\sigma = \sqrt{1/12 \sum_{k=1}^{12} (Y_k^E - Y_k^T)^2}$, where $Y_k^E - Y_k^T$ are the residuals between the observed and calculated monthly averaged station positions for the sinusoid and breather. The shapes of the fitted curves are shown in Fig. 5.

The coincidence of the trajectory shape of measured vertical displacements with the shape of a breather, and the correspondence of the blocky structure in area of GPS site locations to the model of coupled pendulums served as a motivation for application of the sine-Gordon equation to describe the evolution of the vertical components of block movements.

The mathematical model of quasi-periodical vertical components of oscillations of rigidly coupled crustal blocks with the adjacent "hinge"-type faults corresponds to the equation:

$$\frac{\partial^2 \varphi}{\partial \eta^2} - \frac{\partial^2 \varphi}{\partial \xi^2} = \sin \varphi , \qquad (1)$$

$$\eta = \omega t , \xi = x\omega / c , \ \omega^2 = mgl / I , \ c^2 = \tau d^2 / I ,$$

where φ is the angle of deviation of the pendulum (rod) from the equilibrium position; $mgl \sin \varphi$ is the moment of the gravity force, m is the lamped mass of the pendulum, l is the length of the rod (the height of the block), $\tau d^2 \frac{\partial^2 \varphi}{\partial x^2}$ is the sum of the moments of the torsion forces exerted by the adjacent blocks, τ is the constant of the spring torsion (rigidity), d is the increment of the interblock distance (increase or decrease depending on the type of movement), I is the moment of the block inertia.

One of the solutions of equation (1) is called a breather (dynamic soliton) and represents a nonlinear function which, for the case of the soliton with the immobile center of gravity can be written as:

$$\varphi(x,t) = 4 \operatorname{arctg}\left[\left(\frac{\sqrt{1-\omega^2}}{\omega} \right) \frac{\sin(\omega t)}{\operatorname{ch}(x\sqrt{1-\omega^2})} \right], \qquad (2)$$

where ω is the inner frequency of the breather, x determines the origin of the curve and t is the independent variable (time).

Like a soliton, the breather has the shape of an impulse; it is localized in space and is pulsating in time. In the low frequency range $\omega << 1$ the breather can be qualitatively treated as

Nonlin. Processes Geophys. Discuss., doi:10.5194/npg-2016-49, 2016
Manuscript under review for journal Nonlin. Processes Geophys.
Published: 27 September 2016
© Author(s) 2016. CC-BY 3.0 License.

296 a weakly coupled kink-antikink pair (the sine-Gordon equation solutions of opposite signs in the
297 shape of a topological soliton – a wave with a changeless profile in the shape of a kink) (Braun
298 and Kivshar, 2004).
299 The detected high correlation of the observed site displacement trajectories with the
300 theoretical curve corresponding to a breather allows us to suggest that the mechanism of these
301 oscillations can be associated with the occurrence of strain waves in the fault intersection system.
302 In this case, these waves can be qualitatively treated as standing waves of compression-extension
303 in the blocky geological medium.
304 The sine-Gordon equation solution in the shape of a breather has previously been applied
305 for modeling the wave dynamics of faults and strain waves (Mikhailov and Nikolaevskiy, 2000;
306 Gershenzon et al., 2009; Erickson et al., 2011). Mikhailov and Nikolaevskiy (2000) considered a
307 scenario when collision of two tectonic waves (kink-antikink collision) resulted in the
308 occurrence of large earthquake. The solution in the shape of a breather has also been applied for
309 the interpretation of the features of fault dynamics observed after the 1989 Loma-Prieta
310 earthquake (Gershenzon et al., 2009). Based on a modified Burridge–Knopoff model, the
311 solution has been obtained that corresponds to a localized failure – a breather that propagates
312 along a fault and is damping in the fault segment of the final length (Erickson et al., 2011). Wu
313 and Chen (1998) have earlier reduced a one-dimensional Burridge–Knopoff spring-block model
314 to the sine-Gordon equation and applied its solution in the shape of a solitary wave (kink) to
315 investigate earthquakes.
316
317 **6 Concluding remarks**
318
319 The accumulated facts indicate to the propagation of slow wave-like movements within the
320 crust and the lithosphere at different velocities on global and regional scales (Bykov, 2014). The
321 results of our investigation (the periodicity of the seismic components, spatial cycles with phase
322 shift of seismicity maxima, migration velocity of earthquake epicenters) and their comparison
323 with the known data allow us to identify the dynamics of seismicity along the northern boundary
324 of the Amurian plate as a wave process. We have revealed synchronous quasi-periodic seismicity
325 variations in equally spaced clusters with spatial periods of 7.26° and 3.5°, that are comparable
326 with the length of slow strain waves (λ=250-450 km), detected in the Eurasian and Amurian
327 tectonic plate interaction area (107°E-140°E) (Sherman, 2013). The slow strain wave velocity in
328 Pribaikalya and Priamurye attains to 5-20 km/yr and is comparable with the migration velocity
329 of crustal deformations (10-100 km/yr) from the Japan-Kuril-Kamchatka subduction zone (Ishii
330 et al., 1978; Kasahara, 1979; Yoshioka et al., 2015).

Nonlin. Processes Geophys. Discuss., doi:10.5194/npg-2016-49, 2016
Manuscript under review for journal Nonlin. Processes Geophys.
Published: 27 September 2016
© Author(s) 2016. CC-BY 3.0 License.

The calculated average displacement rate value of the maxima of weak seismicity (2≤M≤4) along the northern boundary of the Amurian plate is about 2.7 km/day (~1000 km/yr), which is two orders of magnitude larger than the velocity of slow strain waves (~10-100 km/yr). This may imply that slow strain waves modulate variations of weak seismicity (2≤M≤4) during the year.

The displacement of seismicity in the annual cycles occurs from east to west and coincides with the direction of migration of large earthquakes, strain wave fronts and crustal deformation detected from direct deformographic and GPS measurements (Kasahara, 1979; Bella et al., 1990; Harada et al., 2003; Yoshioka et al., 2015). The slow strain wave fronts are triggers of large earthquakes (M>6) in the submeridional faults of the Amurian plate.

The spatial correlation of migration of seismicity and deformations as well as the migration of deformations – two different manifestations of the geodynamic process – may mean that seismicity migration is associated with the propagation of tectonic stresses in the form of slow strain waves that cause a complementary load and subsequent earthquake occurrence. The numerous results of observations of seismicity migration are hard to explain by other causes rather than wave-like variations of the global and local stress fields.

The conclusions on the wave pattern of the deformation process are consistent with the results of special experimental observations performed to explore crustal block interaction. The seasonal course of displacements of GPS stations NRGR and NRG2, involved in the in situ experimental observations, or of the deformations of the blocky structure of the crust, exhibits a wave-like rather than a linear pattern. The wave-like displacements can be explained by transmittance of slow strain waves.

Resting upon the statistical modeling, we have established the in-phase and anti-phase changes of the components of the full displacement vector, the relative time delay of the maxima and minima for separate components, and dissimilarity of the displacement trajectory from a sinusoid. In order to describe the evolution of oscillations of the interacting blocks, a simple mathematical model is proposed from which it follows the explanation of the observed specific behavior of these blocks.

Based on experimental observation data and the developed model of crustal block movement, we have shown that there is one possible interpretation for this fact that the trajectory of GPS station position disturbance is induced by migrating of crustal deformation in the form of slow waves.

Acknowledgements. The reported study was funded by RFBR according to the research project No. 16-05-00097 a.

Nonlin. Processes Geophys. Discuss., doi:10.5194/npg-2016-49, 2016
Manuscript under review for journal Nonlin. Processes Geophys.
Published: 27 September 2016
© Author(s) 2016. CC-BY 3.0 License.

References

Anderson, D.L.: Accelerated plate tectonics, Science, 187, 1077-1079, 1975.

Barabanov, V.L., Grinevsky, A.O., Kissin, I.G., and Mil'kis, M.P.: Hydrogeological and seismic effects of deformational waves in the foremost Kopet Dag fault zone, Izvestiya Akademii Nauk SSSR. Fizika Zemli, 5, 21-31, 1988.

Bazavluk, T.A. and Yudakhin, F.N.: Deformation waves in Earth crust of Tien Shan on seismological data, Dokl. Akad. Nauk, 329, 565-570, 1993.

Bella, F., Biagi, P.F., Caputo, M., Della, Monica G., Ermini, A., Manjgaladze, P., Sgrigna, V., and Zilpimian, D.: Very slow-moving crustal strain disturbances, Tectonophysics, 179, 131-139, 1990.

Bormotov, V.A. and Bykov, V.G.: Seismological monitoring of the deformation process, Geology of the Pacific Ocean, 16, 981-994, 2001.

Bott, M.H.P. and Dean, D.S.: Stress diffusion from plate boundaries, Nature, 243, 339-341, 1973.

Braun, O.M. and Kivshar, Y.S.: The Frenkel-Kontorova model: concepts, methods, and applications, Berlin: Springer, 2004.

Bykov, V.G.: Strain waves in the Earth: Theory, field data, and models, Russian Geology and Geophysics, 46, 1158-1170, 2005.

Bykov, V.G.: Stick-slip and strain waves in the physics of earthquake rupture: experiments and models, Acta Geophysica, 56, 270-285, 2008.

Bykov, V.G.: Sine-Gordon equation and its application to tectonic stress transfer, Journal of Seismology, 18, 497-510, 2014.

Elsasser, W.M.: Convection and stress propagation in the upper mantle, in: The Application of Modern Physics to the Earth and Planetary Interiors, edited by: Runcorn, S.K., pp. 223-246, Wiley-Interscience, New York, 1969.

Erickson, B.A., Birnir, B., and Lavallee, D.: Periodicity, chaos and localization in a Burridge–Knopoff model of an earthquake with rate-and-state friction, Geophys. J. Intern., 187, 178-198, 2011.

Gorbunova, E.A. and Sherman, S.I.: Slow deformation waves in the lithosphere: Registration, parameters, and geodynamic analysis (Central Asia), Russian J. Pacific Geology, 6, 13-20, 2012.

Gershenzon, N.I., Bykov, V.G., and Bambakidis, G.: Strain waves, earthquakes, slow earthquakes, and afterslip in the framework of the Frenkel-Kontorova model, Physical Review. E, 79, 056601, 2009.

© Author(s) 2016. CC-BY 3.0 License.

401 Harada, M., Furuzawa, T., Teraishi, M., and Ohya, F.: Temporal and spatial correlations of the
402 strain field in tectonic active region, southern Kyusyu, Japan, Journal of Geodynamics, 35,
403 471-481, 2003.
404 Ida, Y.: Slow-moving deformation pulses along tectonic faults, Phys. Earth Planet. Inter., 9, 328-
405 337, 1974.
406 Imaeva, L.P., Imaev, V.S., and Koz'min, B.M.: Seismogeodynamics of the Aldan-Stanovoi block,
407 Russian J. Pacific Geology, 6, 1-12, 2012.
408 Ishii, H., Sato, T., Tachibana, K., Hashimoto, K., Murakami, E., Mishina, M., Miura, S., Sato, K.,
409 and Takagi, A.: Crustal strain, crustal stress and microearthquake activity in the northeastern
410 Japan arc, Tectonophysics, 97, 217-230, 1983.
411 Kasahara, K.: Migration of crustal deformation, Tectonophysics, 52, 329-341, 1979.
412 Kissin, I.G.: Hydrological effects of deformation waves in the Earth's crust, Geophysical
413 Research, 9, 43-52, 2008. (In Russian)
414 Kuz'min, Y.O.: Deformation autowaves in fault zones, Izv. Phys. Solid Earth, 48, 1-16, 2012.
415 Lee, W.H.K., Celebi, M., Todorovska, M.I., and Igel, H. (Eds): Special Issue on "Supplement.
416 Rotational seismology and engineering applications", Bull. Seism. Soc. Am., 99, 1486 p.,
417 2009.
418 Lukk, A.A. and Nersesov, I.L.: Time-dependent parameters of a seismotectonic process,
419 Izvestiya Akademii Nauk SSSR. Fizika Zemli, 3, 10-27, 1982.
420 Malamud, A.S. and Nikolaevskii, V.N.: The periodicity of Pamirs-Hindukush earthquakes and
421 the tectonic waves in subducted lithosphere plates, Dokl. Akad. Nauk. SSSR, 269, 1075-
422 1078, 1983.
423 Malamud, A.S. and Nikolaevsky, V.N.: Cyclicity of seismotectonic events in the marginal
424 region of the Indian lithospheric plate, Dokl. Akad. Nauk. SSSR, 282, 1333-1337, 1985.
425 Mikhailov, D.N. and Nikolaevskiy, V.N.: Tectonic waves of the rotational type generating
426 seismic signals, Izv. Phys. Solid Earth, 36, 895-902, 2000.
427 Milyukov, V., Mironov, A., Kravchuk, V., Amoruso, A., and Crescentini, L.: Global
428 deformations of the Eurasian plate and variations of the Earth rotation rate, Journal of
429 Geodynamics, 67, 97-105, 2013.
430 Miura, S., Ishii, H., and Takagi, A.: Migration of vertical deformations and coupling of
431 island arc plate and subducting plate, in: Slow Deformation and Transmission of Stress in the
432 Earth, edited by: Cohen, S.C. and Vaníiek, P., pp. 125-138, Washington, D.C. Geophysical
433 Monograph Series, 49, 1989.
434 Nevskii, M.V., Morozova L.A., and Zhurba, M.N.: The effect of propagation of the long-period
435 strain perturbations, Dokl. Akad. Nauk SSSR, 296, 1090-1094, 1987.

© Author(s) 2016. CC-BY 3.0 License.

436 Nersesov, I.L., Lukk, A.A., Zhuravlev, V.I., and Galaganov, O.N.: On propagation of strain
437 waves in the crust of southern Central Asia, Izvestiya Akademii Nauk SSSR. Fizika Zemli, 5,
438 102-112, 1990.
439 Nikolaevskiy, V.N.: Geomechanics and fluidodynamics, Kluwer, Dordrecht, 1996.
440 Nikolaevskiy, V.N.: Tectonic stress migration as nonlinear wave process along earth crust faults,
441 in: Proc. of 4th Inter. Workshop on Localization and Bifurcation Theory for Soils and Rocks,
442 Gifu, Japan, 28 Sept. - 2 Oct. 1997, edited by: Adachi, T., Oka, F., and Yashima, A., 137-142,
443 Balkema, Rotterdam, 1998.
444 Press, F. and Allen, C.: Patterns of seismic release in the southern California region, J. Geophys.
445 Res., 100, 6421-6430, 1995.
446 Reuveni, Y., Kedar, S., Moore, A., and Webb, F.: Analyzing slip events along the Cascadia
447 margin using an improved subdaily GPS analysis strategy, Geophys. J. Intern., 198, 1269-
448 1278, 2014.
449 Scholz, C.H.: A physical interpretation of the Haicheng earthquake prediction, Nature, 267, 121-
450 124, 1977.
451 Sherman, S.I.: Deformation waves as a trigger mechanism of seismic activity in seismic zones of
452 the continental lithosphere, Geodynamics & Tectonophysics, 4, 83-117, 2013.
453 Sherman, S.I., Sorokin, A.P., Sorokina, A.T., Gorbunova, E.A., and Bormotov, V.A.: New data
454 on the active faults and zones of modern lithosphere destruction in the Amur region, Doklady
455 Earth Sciences, 439, 1146-1151, 2011.
456 Stein, R.S., Barka, A.A., and Dieterich, J.H.: Progressive failure on the North Anatolian fault
457 since 1939 by earthquake stress triggering, Geophys. J. Intern., 128, 594-604, 1997.
458 Teisseyre, R., Takeo, M., and Majewski, E. (Eds): Earthquake source asymmetry, structural
459 media and rotation effects, Springer-Verlag, Berlin, 2006.
460 Trofimenko, S.V.: Tectonic interpretation of the statistical model of distributions of anomalies
461 azimuths of gravity and magnetic fields of the Aldanian Shield, Pacific Geology, 29, 64-77,
462 2010. (In Russian)
463 Trofimenko, S.V. and Bykov, V.G.: The model of crustal block movement in the South Yakutia
464 geodynamic testing area based on GPS data, Russian J. Pacific Geology, 8, 247-255, 2014.
465 Trofimenko, S.V., Bykov, V.G., and Merkulova, T.V.: Seismicity Migration in the Zone of
466 Convergent Interaction between the Amur Plate and the Eurasian Plate, Journal of
467 Volcanology and Seismology, 9, 210-222, 2015.
468 van Dam, T.M., Blewitt, G., and Heflin, M.B.: Atmospheric pressure loading effects on global
469 positioning system coordinate determinations, J. Geophys. Res., 99, 23939-23950, 1994.

Nonlin. Processes Geophys. Discuss., doi:10.5194/npg-2016-49, 2016
Manuscript under review for journal Nonlin. Processes Geophys.
Published: 27 September 2016
© Author(s) 2016. CC-BY 3.0 License.

470 Wang, S. and Zhang, Z.: Plastic-flow waves ("slow-waves") and seismic activity in Central-
471 Eastern Asia, Earthquake Research in China, 19, 74-85, 2005.
472 Wu, Z.L. and Chen, Y.T.: Solitary wave in a Burridge-Knopoff model with slip-dependent
473 friction as a clue to understanding the mechanism of the self-healing slip pulse in an
474 earthquake rupture process, Nonlin. Processes Geophys., 5, 121-125, 1998.
475 Yoshioka, S., Matsuoka, Y., and Ide, S.: Spatiotemporal slip distributions of three long-term
476 slow slip events beneath the Bungo Channel, southwest Japan, inferred from inversion
477 analyses of GPS data, Geophys. J. Intern., 201, 1437-1455, 2015.
478
479
480
481
482
483
484
485
486
487
488
489
490
491
492
493
494
495
496
497
498
499
500
501
502
503
504
505
506
507
508
509
510
511
512
513
514
515
516
517

Nonlin. Processes Geophys. Discuss., doi:10.5194/npg-2016-49, 2016
Manuscript under review for journal Nonlin. Processes Geophys.
Published: 27 September 2016
© Author(s) 2016. CC-BY 3.0 License.

518 **Figures**

519

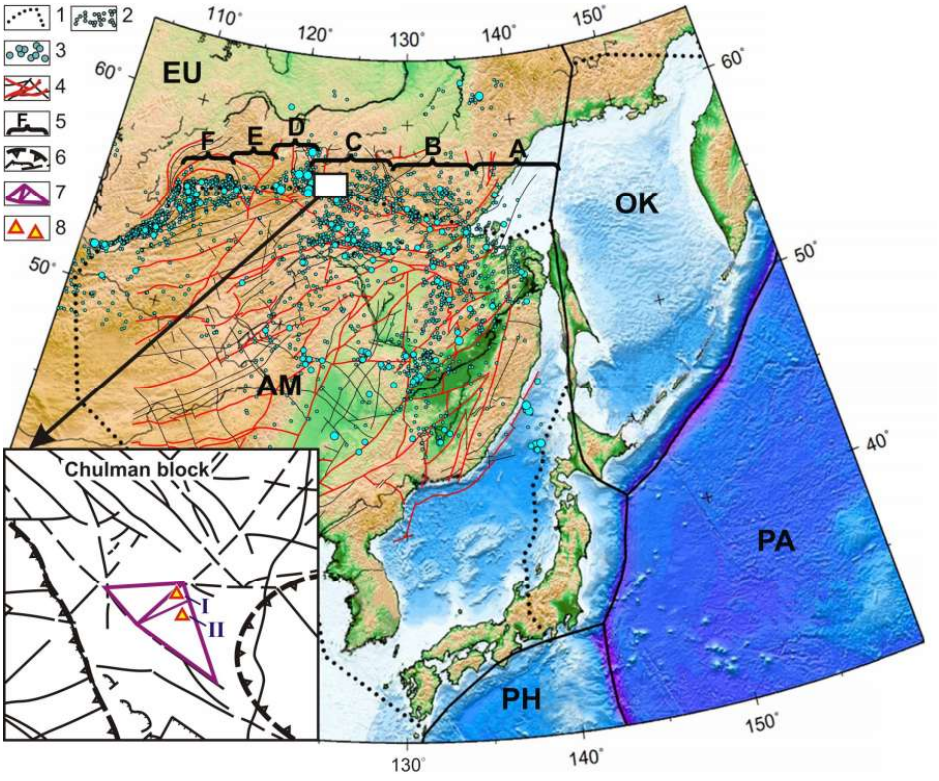

520

521 **Fig. 1.** The distribution of earthquake epicenters in the zone of interaction between the Amurian,
522 Eurasian and Okhotsk lithospheric plates.
523 1 – lithospheric plate boundaries: EU - Eurasian PA - Pacific, PH - Philippine, OK – Okhotsk; 2
524 – epicenters of earthquakes with magnitude M>3; 3 - epicenters of earthquakes with magnitude
525 M>5; 4 – main tectonic faulting; 5 – spatial cycles of seismicity.
526 A black rectangle shows a sketch map of fault tectonics of the Chulman block, where GPS sites
527 are located: 6 – northeast- and northwest-trending faults of different kinematics; 7 – local block,
528 bordered by active faults; 8 – GPS sites (I – NRGR, II – NRG2).
529
530
531
532
533
534
535
536
537
538
539
540

Nonlin. Processes Geophys. Discuss., doi:10.5194/npg-2016-49, 2016
Manuscript under review for journal Nonlin. Processes Geophys.
Published: 27 September 2016
© Author(s) 2016. CC-BY 3.0 License.

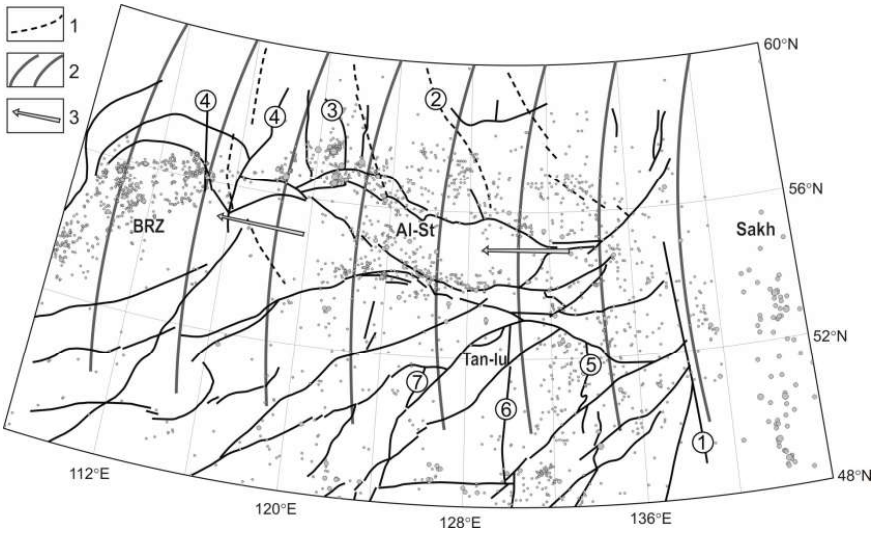

Fig. 2 The spatial distribution of seismicity in the annual cycles with respect to the strain wave fronts and meridional structures.
Active tectonic faulting: Tan-Lu fault zone, Aldan-Stanovoy block (Al-St) and Baikal rift zone (BRZ). Figures in the circles denote the faults: 1 - Limurchan, 2 - Tyrkanda, 3 – Temulyakit meridional faults, 4 – meridional structures of the eastern flank of the Baikal rift zone, 5 – Gastakh, 6 – West-Turanian, 7 – Levo-Minsky.
1 – submeridional interblock faults of the Aldan shield; 2 – strain wave fronts (Sherman, 2013); 3 – the direction of seismicity maxima migration in the annual cycles and movements of the strain wave fronts.

Nonlin. Processes Geophys. Discuss., doi:10.5194/npg-2016-49, 2016
Manuscript under review for journal Nonlin. Processes Geophys.
Published: 27 September 2016
© Author(s) 2016. CC-BY 3.0 License.

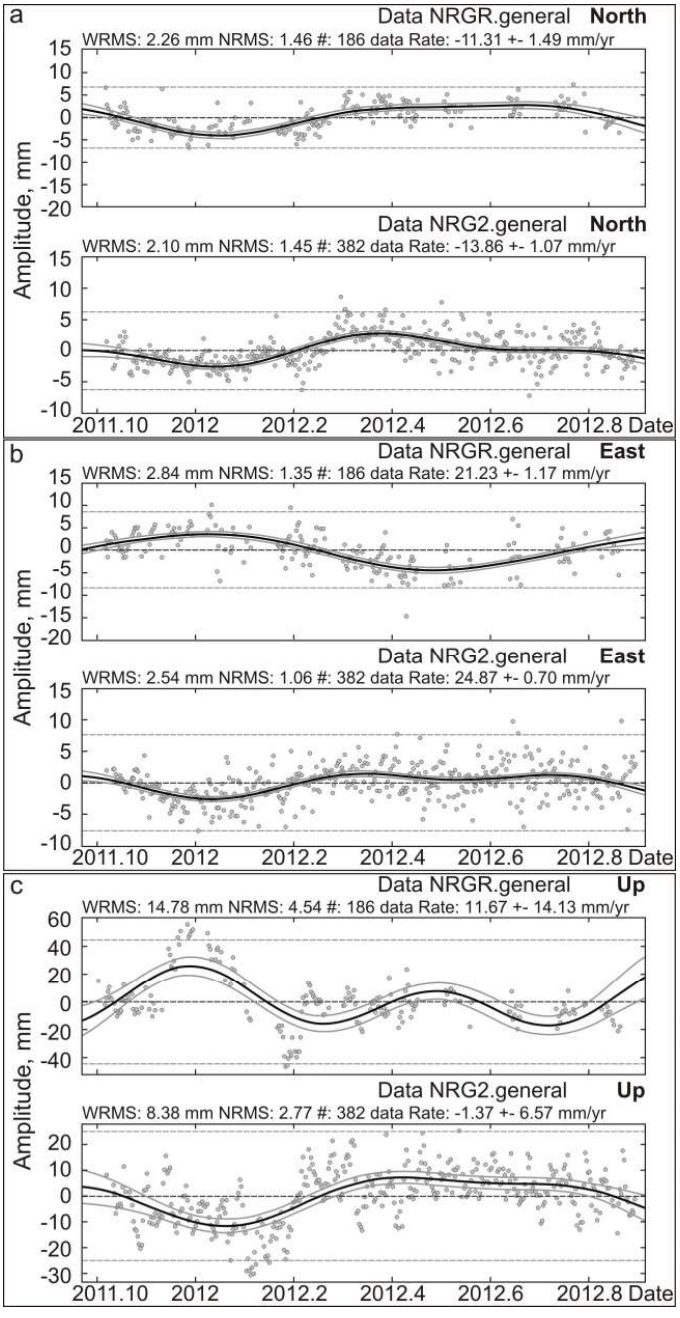

Fig. 3 The dynamics of displacement components of NRGR and NRG2 station daily positions in different directions.
a – for the N–S components; b – for the E–W components; c – for the vertical (Up–Down) components.

Nonlin. Processes Geophys. Discuss., doi:10.5194/npg-2016-49, 2016
Manuscript under review for journal Nonlin. Processes Geophys.
Published: 27 September 2016
© Author(s) 2016. CC-BY 3.0 License.

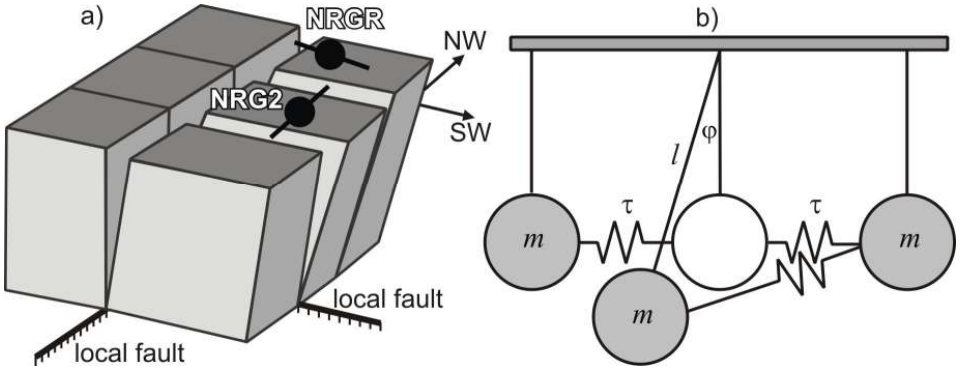

Fig. 4 The generalized model of block movement in the vertical plane along differently oriented local faults of the hinge type due to variable vertical loading. (a) The model of block movement along NE- and NW-trending faults and schemes of the full displacement vector decomposition into components. (b) The model of block movement in the shape of coupled pendulums (notations are given in the text).

Nonlin. Processes Geophys. Discuss., doi:10.5194/npg-2016-49, 2016
Manuscript under review for journal Nonlin. Processes Geophys.
Published: 27 September 2016
© Author(s) 2016. CC-BY 3.0 License.

Nonlinear Processes in Geophysics
Discussions
Open Access
EGU

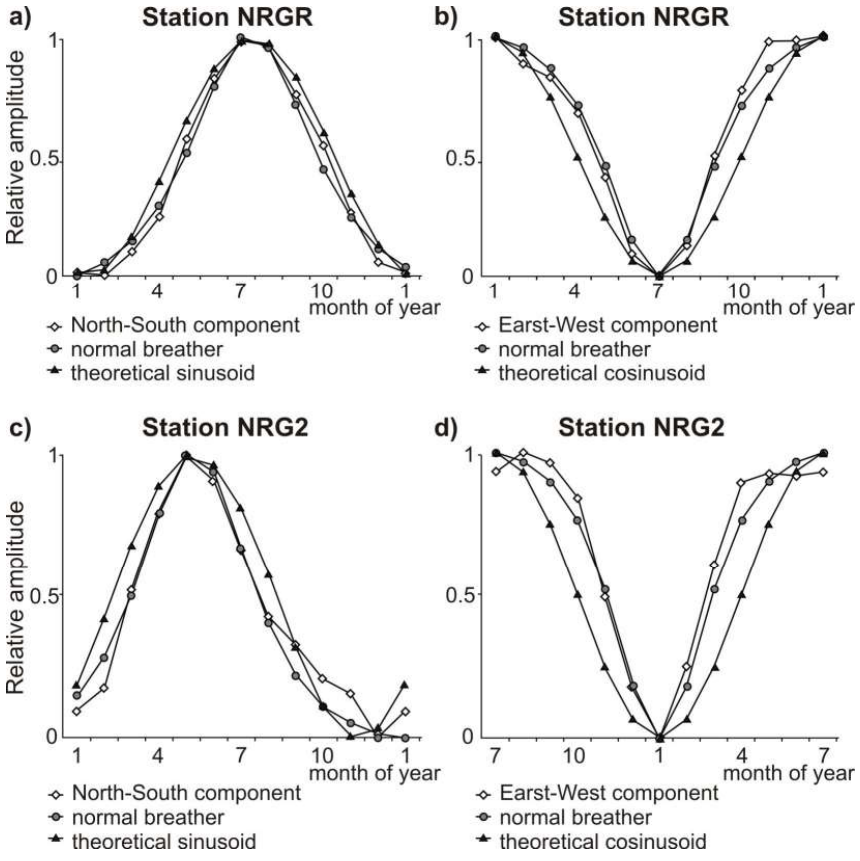

596

597 **Fig. 5** Seasonal variations of NRGR and NRG2 station positions.
598 Approximation of the observed displacement curves by the theoretical curves for the N–S (a) and
599 E–W (b) components at the NRGR site; for the N–S (c) and E–W (d) components at the NRG2
600 site.
601